

# Heavy Flavor Production and Spectroscopy with CDF

Prabhakar Palni, on behalf of the CDF Collaboration<sup>a</sup>
<sup>a</sup>Department of Physics and Astronomy, University of New Mexico, MSC07 4220, 1919 Lomas Blvd. NE, Albuquerque, NM 87131-0001, USA

## Abstract

Using data from  $p\bar{p}$  collisions at  $\sqrt{s} = 1.96$  TeV recorded by the CDF II detector at the Fermilab Tevatron, we present three recent results on heavy flavor production: an observation of the excited resonance state  $\Lambda_b^{*0}$  in its fully reconstructed decay mode to  $\Lambda_b^0\pi^+\pi^-$ , a study of quark fragmentation using kaons produced in association with prompt  $D_s^\pm/D^\pm$  mesons, and the measurement of angular distributions of muons from  $\Upsilon(1S, 2S, 3S)$  decays in both the Collins-Soper and the  $s$ -channel helicity frames.

## 1. Observation of the bottom baryon resonance $\Lambda_b^{*0}$

Baryons with a heavy quark  $Q$  as the nucleus and a light diquark  $q_1q_2$  as the two orbiting electrons can be viewed as the helium atoms of QCD. The heavy quark in the baryon may be used as a probe of confinement which allows the study of non-perturbative QCD in a different regime from that of the light baryons.

The models that describe the heavy hadron's spectroscopy in the frameworks of Heavy Quark Effective Theories (HQET) [1] treat the heavy baryon as a system of a heavy quark  $Q$  considered as a static color source with mass  $m_Q \gg \Lambda_{QCD}$  and a light diquark  $qq$  with a gluon field [2]. As the spin  $S_{qq}$  of the light diquark and the spin  $S_Q$  of the heavy quark are decoupled in HQET, heavy baryons can be described by the quantum numbers  $S_Q, m_Q, S_{qq}$ , and  $m_{qq}$ .

The total spins of the  $S$ -wave (no orbital excitations) baryon multiplets can be expressed as the sum  $J = S_Q + S_{qq}$ . Then the singlet  $\Lambda_b^0$  baryon, with quark content  $b[ud]$  according to HQET, has spin of the heavy quark  $S_b^P = \frac{1}{2}^+$  and isospin  $I = 0$ . Its flavor antisymmetric  $[ud]$  diquark has spin  $S_{[ud]}^P = 0^+$  [3]. Under these conditions the  $b$  quark and the  $[ud]$  diquark make the lowest-lying singlet ground state  $J^P = \frac{1}{2}^+$ . The partner of the  $\Lambda_b^0$  baryon in the charm quark sector is the  $\Lambda_c^+$  baryon.

Once the  $[ud]$  diquark acquires an orbital excitation with  $L = 1$  relative to the heavy quark  $b$ , two excited states  $\Lambda_b^{*0}$  emerge with the same quark content as the

singlet  $\Lambda_b^0$ , with isospin  $I = 0$  but with total spin  $J^P = \frac{1}{2}^-$  or  $J^P = \frac{3}{2}^-$ . These isoscalar states are the lowest lying  $P$ -wave states that can decay to the singlet  $\Lambda_b^0$  via strong processes involving emission of a pair of soft pions if parity  $P$  is conserved and provided sufficient phase space is available. Both  $\Lambda_b^{*0}$  particles are classified as bottom baryon resonant states.

LHCb has reported the first observation of two narrow structures at 5912 MeV/ $c^2$  and 5920 MeV/ $c^2$  [4] in the invariant mass spectrum of  $\Lambda_b\pi^+\pi^-$ . These structures are interpreted as the orbitally excited  $\Lambda_b^{*0}(5912)$  and  $\Lambda_b^{*0}(5920)$  bottom baryon resonances. Using a data sample of 9.6 fb<sup>-1</sup> collected with the CDF II detector [5], we undertake a search for the resonant states produced at the Tevatron and decaying in the same mode,  $\Lambda_b\pi^+\pi^-$  [6].

This analysis is based on a CDF data set equivalent to 9.6 fb<sup>-1</sup> collected with the displaced two-track trigger [7] between March 2002 and December 2011. We search for  $\Lambda_b^{*0}$  states in the exclusive strong decay mode  $\Lambda_b^{*0} \rightarrow \Lambda_b\pi^+\pi^-$ , where the pair of low momentum pions  $\pi^+\pi^-$  is produced near the kinematic threshold. The  $\Lambda_b^0$  decays to  $\Lambda_c^+\pi_b^-$ , and this is followed by the weak decay  $\Lambda_c^+ \rightarrow pK^-\pi^+$ . To reconstruct the parent baryons, the tracks of charged particles are combined to form candidates. No particle identification is used in this analysis.

The analysis begins with reconstruction of the  $\Lambda_c^+ \rightarrow pK^-\pi^+$  decay by fitting three tracks to a common ver-

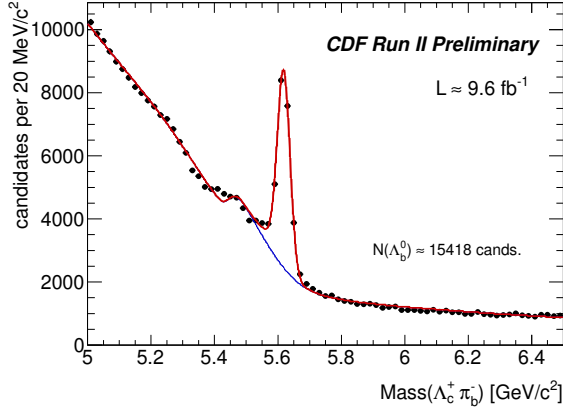


Figure 1: The invariant mass distribution of  $\Lambda_b^{*0} \rightarrow \Lambda_b^0 \pi^+ \pi^-$  candidates with the projection of a mass fit overlaid.

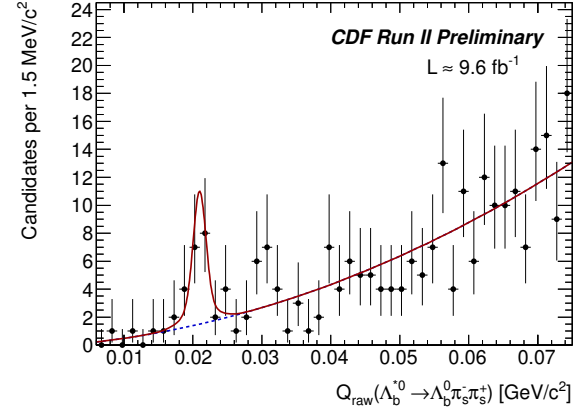


Figure 2: The projection of the unbinned fit for  $Q$  values of the  $\Lambda_b^{*0}$  candidates in the range  $[0.006, 0.075]$   $\text{GeV}/c^2$ .

tex. The invariant mass of the  $\Lambda_c^+$  candidate is required to be within  $\pm 18 \text{ MeV}/c^2$  of the world-average  $\Lambda_c^+$  mass [8]. The momentum vector of the  $\Lambda_c^+$  candidate is then extrapolated to intersect with a fourth track that is assumed to be the pion, to form the  $\Lambda_b^0 \rightarrow \Lambda_c^+ \pi^-$  candidate. The  $\Lambda_b^0$  vertex is subjected to a three-dimensional kinematic fit with the  $\Lambda_c^+$  candidate mass constrained to its world average value. The small bump below the  $\Lambda_b^0$  signal corresponds to fully reconstructed  $B$  meson decays that pass the  $\Lambda_b^0 \rightarrow \Lambda_c^+ \pi^-$  selection criteria.

To reduce combinatorial background and contributions from partially reconstructed decays, CDF requires  $\Lambda_b^0$  candidates to point to the primary vertex by requiring the impact parameter  $d_0(\Lambda_b^0)$  not to exceed  $80 \mu\text{m}$ . The  $\Lambda_b^0$  candidate must have transverse momentum  $p_T(\Lambda_b^0)$  greater than  $9.0 \text{ GeV}/c$  to ensure that the slow pions from the  $\Lambda_b^0$  decay are within the kinematic acceptance of the track reconstruction. Figure 1 shows a prominent  $\Lambda_b^0$  signal in the  $\Lambda_c^+ \pi^-$  invariant mass distribution. A binned maximum-likelihood fit finds a signal of approximately 15,400 candidates at the expected  $\Lambda_b^0$  mass, with a signal to background ratio of around 1.1. To reconstruct the  $\Lambda_b^{*0} \rightarrow \Lambda_b^0 \pi^+ \pi^-$  candidates, each  $\Lambda_c^+ \pi^-$  candidate with an invariant mass within the  $\Lambda_b^0$  signal region,  $5.561 - 5.677 \text{ GeV}/c^2$ , is combined with a pair of oppositely charged tracks. The  $\Lambda_b^0$  mass range covers  $\pm 3$  standard deviations as determined by a fit to the signal peak of Figure 1.

To suppress systematic uncertainties, the analysis uses the mass difference  $Q$ , which is defined as  $Q \equiv M(\Lambda_b^{*0} \rightarrow \Lambda_b^0 \pi^+ \pi^-) - M(\Lambda_b^0) - 2m(\pi^\pm)$ . Figure 2 shows the result of a maximum likelihood fit to the unbinned  $Q$ -value distribution of  $\Lambda_b^{*0}$  overlaid

to data. A narrow structure at  $Q \sim 21 \text{ MeV}/c^2$  is clearly seen. The fit finds  $17.3^{+5.3}_{-4.6}$  signal candidates at  $Q = 20.68 \pm 0.35 \text{ MeV}/c^2$ , where the resulting  $Q$  value is adjusted with the calibrated scale offset of  $-0.28 \text{ MeV}/c^2$ . From the measured  $\Lambda_b^{*0}$   $Q$  value we extract the absolute masses using the known value of the  $\pi^\pm$  mass [8] and the CDF  $\Lambda_b^0$  mass measurement,  $M(\Lambda_b^0) = 5619.7 \pm 1.2 (\text{stat}) \pm 1.2 (\text{syst}) \text{ MeV}/c^2$ , as obtained in an independent sample. The  $\Lambda_b^{*0}$  mass is found to be  $M(\Lambda_b^{*0}) = 5919.5 \pm 0.35 (\text{stat}) \pm 1.72 (\text{syst}) \text{ MeV}/c^2$ . The  $\Lambda_b^0$  statistical and systematic uncertainties contribute to the systematic uncertainty on the  $\Lambda_b^{*0}$  absolute mass.

The local significance of the signal is  $4.6\sigma$ . The significance of the signal for the search region of  $6 - 50 \text{ MeV}/c^2$  is  $3.5\sigma$ . The CDF result confirms the  $\Lambda_b^{*0}(5920)$  state recently observed by the LHCb Collaboration. We do not observe the  $\Lambda_b^{*0}(5912)$  resonance state observed by the LHCb Collaboration because of our low detector acceptance to slow pions. The result is consistent with theoretical predictions.

## 2. Quark fragmentation study using kaons produced in association with prompt $D_s^\pm/D^\pm$ mesons

CDF probes the non-perturbative aspects of quark fragmentation by measuring the quark flavor fractions of charged particles produced in association with  $D_s^\pm$  and  $D^\pm$  mesons. Since QCD locally conserves quark flavor, this probes new details of the process by which quark anti-quark pairs are produced and subsequently form bound states in the fragmentation of a heavy quark

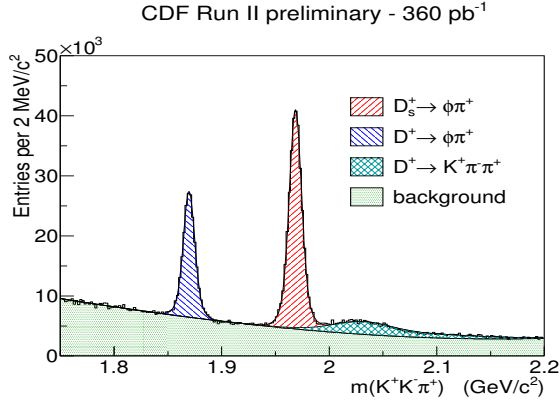


Figure 3: The invariant mass projections obtained from the likelihood fit performed in the lowest  $p_T(KK\pi)$  bin.

jet. CDF performs an analysis to study kaon production around charm mesons, namely  $D_s^\pm$  and  $D^\pm$  [9]. According to the naive fragmentation model, a kaon will be produced in the first fragmentation branch in association with a  $D_s^\pm$ , whereas creation of a  $D^\pm$  meson results in the production of a pion in the first fragmentation branch. Hence, more opposite-charge kaons are likely to be produced around  $D_s^\pm$  than  $D^\pm$ . In this study, we provide a comparison of the kinematical distributions of kaons produced around prompt  $D_s^\pm$  and prompt  $D^\pm$  that allows us to extract some information about the properties of the kaon that is most likely to be produced in the first fragmentation branch. We compare the results in data with predictions by the PYTHIA event generator [10] (which uses the string fragmentation model [11]) and with predictions by the HERWIG event generator [12] (which uses the cluster fragmentation model [13]).

Using a sample of events collected with a displaced two-track trigger [7], CDF reconstructs  $D_s^\pm/D^\pm \rightarrow \phi\pi^\pm$ ,  $\phi \rightarrow K^+K^-$  decays and analyzes events that have invariant mass in the range  $1.75 < m(KK\pi) < 2.2$   $\text{GeV}/c^2$ . The particular trigger requires a pair of oppositely charged tracks with  $p_T > 2.0$   $\text{GeV}/c$  and impact parameter  $d_0 > 120$   $\mu\text{m}$ . The sum of their transverse momentum has to be greater than  $5.5$   $\text{GeV}/c$ . This event sample, obtained from  $360$   $\text{pb}^{-1}$  of data set, contains about 260,000  $D_s^\pm$  and 140,000  $D^\pm$  candidates with transverse momentum in the range  $7 < p_T(KK\pi) < 30$   $\text{GeV}/c$ .

To extract information pertaining to charm quark fragmentation, we concentrate on the prompt  $D_s^\pm/D^\pm$  component. We use the impact parameter distribution of the reconstructed  $KK\pi$  candidates to statistically sep-

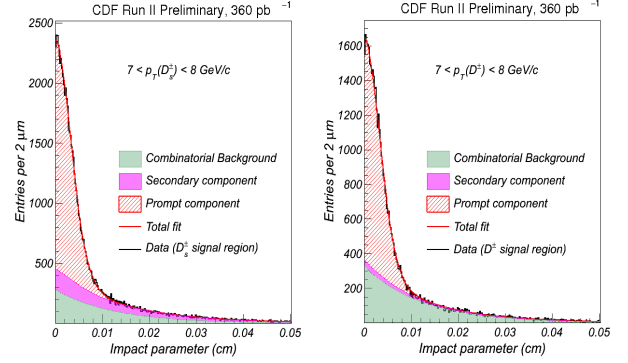


Figure 4: The impact parameter projections obtained from the likelihood fit performed in the lowest  $p_T(KK\pi)$  bin.

arate the prompt and secondary  $D$  components in data. We use two particle identification techniques to measure the kaon, pion, and proton fractions around the various  $D$  components. These are the measurement of the specific ionization per unit track length ( $dE/dx$ ) in the central tracking drift chamber and the time of flight of the particle measured in the Time-of-Flight (TOF) sub-detector. The silicon vertex trigger system has excellent impact parameter resolution of  $35$   $\mu\text{m}$  ( $50$   $\mu\text{m}$  when convoluted with a contribution from the beamspot).

A prompt  $D_s^\pm/D^\pm$  meson that is created during hadronization of the charm quark should ideally have a zero impact parameter with respect to the primary vertex. However, due to the finite resolution of the detector, the impact parameter distribution of the prompt component will follow a Gaussian distribution with the width of the Gaussian being equal to the detector resolution. A secondary  $D_s^\pm/D^\pm$  meson that is produced in a  $B$  decay is boosted and can have non zero impact parameter with respect to the primary vertex. This difference in the inherent shape of the impact parameter distribution of the two components measured with respect to the primary vertex can be used to separate the prompt and secondary  $D_s^\pm/D^\pm$  components.

The invariant mass distribution is used to separate the  $D_s^\pm$  and  $D^\pm$  signal from the combinatorial background. The  $D_s^\pm$  and  $D^\pm$  signal peak is described using a double Gaussian function. The shape of the wide bump that occurs around  $2.02$   $\text{GeV}/c^2$  in the invariant mass distribution is obtained using Monte Carlo samples of mis-reconstructed  $D^+ \rightarrow K^-\pi^+\pi^+$ . A fourth order polynomial is used to describe the shape of the background component. The likelihood fit is performed in bins of transverse momentum of the  $KK\pi$  candidate.

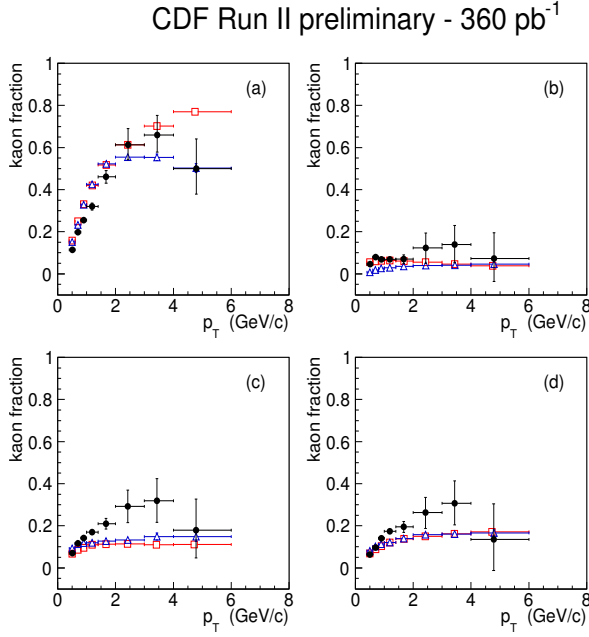


Figure 5: Distribution of kaon fractions measured around prompt  $D_s^\pm/D^\pm$  mesons in bins of transverse momentum  $p_T$  of the maximum- $p_T$  track found in the cone.

The invariant mass projections obtained from the fit are shown in Fig. 3.

The shape of the prompt  $D$  component in the impact parameter distribution is described using a double Gaussian function. In order to describe the shape of the secondary component, we extract the impact parameter distribution of secondary  $D_s^\pm/D^\pm$  mesons using Monte Carlo samples of  $B$  decays. The template that describes the impact parameter distribution for secondary  $D_s^\pm/D^\pm$  is convoluted with the prompt resolution function. The shape of the background component in the impact parameter distribution is obtained empirically. The impact parameter of background is assumed to be independent of mass, so we use the same function to describe the impact parameter of the background component in the sideband regions and under the  $D_s^\pm/D^\pm$  signal peaks, i.e., in the entire mass range  $[1.75, 2.2]$  GeV/ $c^2$ . The impact parameter projections obtained from the likelihood fit to data within  $\pm 3\sigma$  of the  $D_s^\pm/D^\pm$  signal peak are shown in Fig. 4.

We select the maximum- $p_T$  track in a cone of radius  $\Delta R = 0.7$  around the  $(KK\pi)$  candidate, where  $\Delta R = \sqrt{\Delta\eta^2 + \Delta\phi^2}$ ,  $\eta$  is pseudorapidity, and  $\phi$  is an azimuthal angle. This requirement is based on the hypoth-

esis that the maximum- $p_T$  track is most likely to be correlated with the production of a heavy meson in the fragmentation process. Using the sample of maximum- $p_T$  tracks, we measure the kaon fraction around the prompt  $D_s^\pm/D^\pm$  component by performing a multidimensional likelihood fit using four distributions: the invariant mass and impact parameter distributions of the  $(KK\pi)$  candidates and the TOF and  $dE/dx$  distributions of the maximum- $p_T$  track found in the cone around the reconstructed  $(KK\pi)$  candidates.

We measure the kaon fraction around prompt  $D_s^\pm/D^\pm$  mesons for opposite-sign and same-sign charge combinations. In the opposite-sign combination, the track in the cone and the  $D$  candidate are oppositely charged. In this case, we expect the kaon production to be enhanced around prompt  $D_s^\pm$  compared to prompt  $D^\pm$  since formation of a prompt  $D_s^\pm$  meson requires conservation of strangeness in the first fragmentation branch. In the same-sign combination, the track in the cone and the  $D$  candidate have the same charge. In this combination, we expect the kaon production fraction to be similar around both the  $D_s^\pm$  and  $D^\pm$  mesons since same-sign kaons are likely to be produced in later branches of the fragmentation process. In addition to the two charge combinations, we measure the kaon fraction around prompt  $D_s^\pm/D^\pm$  mesons and compare the distribution in data with predictions by the PYTHIA and HERWIG Monte Carlo event generators. This comparison is shown in Fig. 5.

The data indicate that, in the opposite-sign charge combination, kaon production around prompt  $D_s^\pm$  is enhanced compared to production around prompt  $D^\pm$ . In the same-sign charge combination, kaon production around prompt  $D_s^\pm$  and prompt  $D^\pm$  is similar. The enhanced production of oppositely charged kaons around prompt  $D_s^\pm$  mesons is a feature of the phenomenological models used to describe the fragmentation process in Monte Carlo event generators. The results of the comparative study indicate that the  $p_T$  distributions for early fragmentation kaons produced around prompt  $D_s^\pm$  are in better qualitative agreement with predictions of fragmentation models compared to generic kaons that are produced in later fragmentation branches, for which the models underestimate the fraction of kaons.

### 3. Measurement of angular distributions of $\Upsilon(nS) \rightarrow \mu^+\mu^-$ decays

For more than a decade, the description of heavy quarkonia production at hadron colliders has proved to be challenging. Models that were constructed to accommodate the surprisingly large production cross sections of  $J/\psi$  and  $\Upsilon$  mesons also make specific predictions

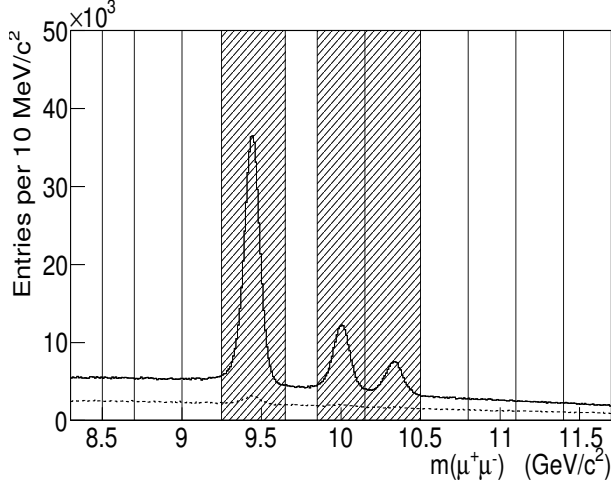


Figure 6: Mass distribution of  $\mu^+\mu^-$  candidates in the prompt (solid line) and displaced (dashed line) samples, with the ranges of invariant mass used to select the signal and sideband events indicated. Hatched regions indicate the three mass ranges containing the  $\Upsilon(nS)$  signals.

about their production polarization but are generally in poor agreement with experimental measurements [14, 15]. Discrepancies between results obtained by different experiments suggest that quarkonia might be strongly polarized when produced, but that different experimental acceptances limit formulation of a complete picture. The angular distribution of muons from  $\Upsilon \rightarrow \mu^+\mu^-$  decays is described in the  $\Upsilon$  rest frame by the distribution

$$\frac{d\Gamma}{d\Omega} \sim 1 + \lambda_\theta \cos^2 \theta + \lambda_\varphi \sin^2 \theta \cos 2\varphi + \lambda_{\theta\varphi} \sin 2\theta \cos \varphi$$

where  $\theta$  is the polar angle measured with respect to the quantization axis,  $\varphi$  is the azimuthal angle measured with respect to the production plane containing the  $\Upsilon$  and the beam axis. Previous experiments have only measured  $\lambda_\theta$  as a function of the  $\Upsilon$  transverse momentum in one reference frame, and significant polarization could be manifest by significantly nonzero values of  $\lambda_\varphi$  or  $\lambda_{\theta\varphi}$  even when  $\lambda_\theta \sim 0$  [16]. The CDF analysis employs a new technique with which to study the angular distribution of muons in  $\Upsilon$  decay and is the first to provide information on all three coefficients, measured in multiple reference frames [17].

Using a sample of events collected with dimuon triggers, we reconstruct oppositely charged muons and analyze those events which have invariant mass in the range  $8.3 < m(\mu^+\mu^-) < 11.7 \text{ GeV}/c^2$ . This event sample, obtained from  $6.7 \text{ fb}^{-1}$  of data set, contains 550,000  $\Upsilon(1S)$ , 150,000  $\Upsilon(2S)$ , and 76,000  $\Upsilon(3S)$  decays. The properties of dimuon candidates that have

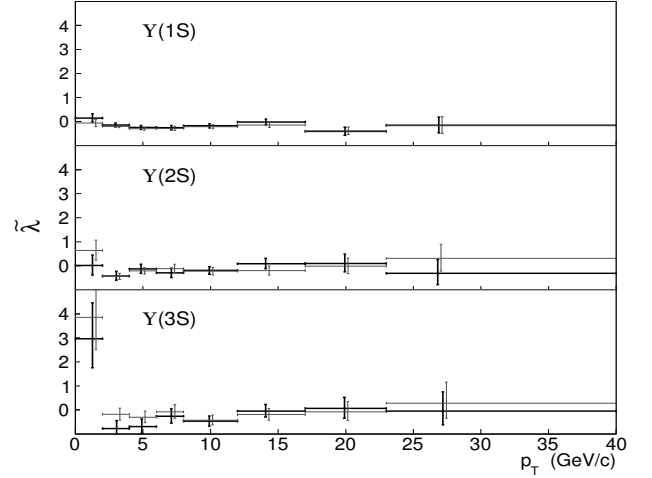


Figure 7: Rotational invariant  $\tilde{\lambda}$  as a function of  $p_T(\Upsilon)$  for the  $\Upsilon(1S)$ ,  $\Upsilon(2S)$ , and  $\Upsilon(3S)$  states

invariant mass near the  $\Upsilon(nS)$  resonances are described using a two-component model for the  $\Upsilon(nS)$  signal itself and the background. The angular distribution of the  $\Upsilon(nS)$  component is extracted from the inclusive sample by means of constraints on the amount of background present in the sample and the angular distribution of the background component. We find that the background is dominated by muons from  $b$ -decays and can be isolated by requiring that one muon is displaced, that is, has an impact parameter inconsistent with production at the primary vertex. We verify that this sample has the same angular distribution as the complementary prompt sample by comparing their angular distributions in mass regions that do not contain  $\Upsilon$  decays.

The angular distribution analysis is performed separately in each of the 12 bins of dimuon mass shown in Fig. 6. The angular distributions of  $\Upsilon$  decays are analyzed in eight bins of  $p_T(\Upsilon)$  from 0 to 40  $\text{GeV}/c$  and are restricted to rapidity  $|\eta(\Upsilon)| < 0.6$ . For a given range of transverse momenta, the sample of dimuon candidates is divided into two subsamples according to whether the trajectory of one of the muons misses the beam axis by a distance  $|d_0| > 150 \mu\text{m}$ . Events with at least one muon satisfying this requirement are referred to as the displaced sample since they are consistent with the presence of a long-lived parent particle, a characteristic feature of the dimuon background arising from semileptonic decays of heavy quarks. These criteria do not bias the angular distribution and, since the displaced sample contains almost no  $\Upsilon$  signal, it provides a good description of the dimuon background that remains in the com-

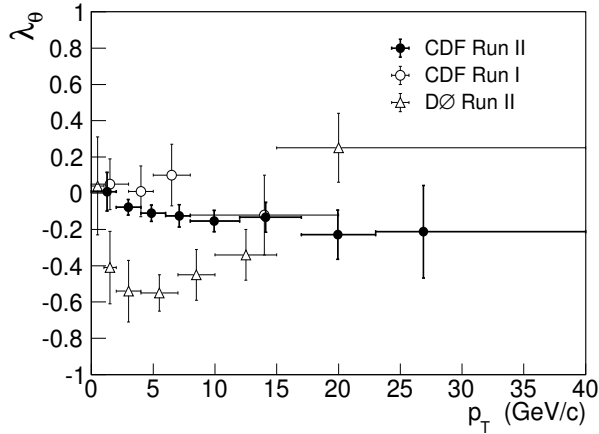


Figure 8: Comparison of the  $\lambda_\theta$  parameter measured for  $\Upsilon(1S)$  decays in the  $s$ -channel helicity frame with previous measurements from the CDF [14] and the D0 [15] experiments.

plementary prompt sample.

Figure 7 shows the rotational invariant  $\tilde{\lambda}$ , which is defined as  $\tilde{\lambda} = \frac{\lambda_\theta + 3\lambda_\phi}{1 - \lambda_\phi}$  as calculated from the measured values of  $\lambda_\theta$  and  $\lambda_\phi$  in each  $p_T$  range for both the Collins-Soper and  $s$ -channel helicity frames. Uncertainties in  $\tilde{\lambda}$  measured in the two coordinate frames are highly correlated. Monte Carlo simulations are used to calculate the expected sizes of differences between the two values of  $\tilde{\lambda}$  and in most cases, the observed deviations are found to be consistent with purely statistical fluctuations. The values of  $\tilde{\lambda}$  suggest that the decays of all three  $\Upsilon(nS)$  resonances are consistent with an unpolarized mixture of states.

Figure 8 shows a comparison of the  $\lambda_\theta$  parameter, measured for the  $\Upsilon(1S)$  state in the  $s$ -channel helicity frame, with previous measurements. The current result is found to be statistically consistent with the previous measurement from CDF [14], which was made for  $|y| < 0.4$  at  $\sqrt{s} = 1.8$  TeV. Restricting the current measurement to  $|y| < 0.4$  does not change the results appreciably. The current  $\Upsilon(1S)$  result is inconsistent with the previous measurement from the D0 experiment [15] at the level of  $4.5\sigma$ .

#### 4. Conclusions

CDF confirms the  $\Lambda_b^{*0}(5920)$  state recently observed by the LHCb Collaboration. The local significance of the signal is  $4.6\sigma$  and the significance of the signal for the search region of  $6 - 50$  MeV/ $c^2$  is  $3.5\sigma$ . The result is consistent with theoretical predictions.

CDF compares the kinematic distribution of the measured kaon fraction around prompt  $D_s^\pm/D^\pm$  mesons with predictions from the string fragmentation model used in the PYTHIA event generator and the cluster fragmentation model used in the HERWIG event generator. The  $p_T$  distribution for early fragmentation kaons produced around prompt  $D_s^\pm$  is in good qualitative agreement with the predictions from the fragmentation models when compared to that of generic kaons that are produced in later fragmentation branches, for which the models underestimate the fraction of kaons.

We have measured the angular distributions of muons from  $\Upsilon(1S)$ ,  $\Upsilon(2S)$ , and  $\Upsilon(3S)$  decays with  $|y| < 0.6$  and in several ranges of transverse momentum up to 40 GeV/ $c$ . We find that the decay-angle distributions of all three  $\Upsilon(nS)$  states are nearly isotropic, as was suggested by previous measurements [14] in the case of the  $\Upsilon(1S)$ . This is the first measurement to simultaneously determine the three parameters needed to fully quantify the angular distribution of  $\Upsilon(nS) \rightarrow \mu^+\mu^-$  decays. This is also the first analysis to present information on the angular distribution of  $\Upsilon(3S)$  mesons produced in high energy  $p\bar{p}$  collisions. A recent CMS analysis employed the same technique and is in agreement with the CDF result [18].

#### References

- [1] M. Neubert, Phys. Rept. **245**, 259 (1994); A. V. Manohar and M. B. Wise, Camb. Monogr. Part. Phys. Nucl. Phys. Cosmol. **10**, 1 (2000).
- [2] N. Isgur and M. B. Wise, Phys. Lett. B **232**, 113 (1989); *Ibid.* **237**, 527 (1990).
- [3] J. G. Korner, M. Kramer, and D. Pirjol, Prog. Part. Nucl. Phys. **33**, 787 (1994).
- [4] R. Aaij *et al.* (LHCb Collaboration), arXiv:1205.3452 [hep-ex].
- [5] D. Acosta *et al.* (CDF Collaboration), Phys. Rev. D **71**, 032001 (2005).
- [6] CDF Collaboration, CDF public note 10900.
- [7] B. Ashmanskas *et al.* (CDF Collaboration), Nucl. Instrum. Meth. A **518**, 532-536 (2004).
- [8] J. Beringer *et al.*, Phys. Rev. D **86**, 010001 (2012).
- [9] CDF Collaboration, CDF public note 10704.
- [10] T. Sjostrand *et al.*, A Brief Introduction to PYTHIA 8.1, LU TP 07-28, October 2007.
- [11] B. Andersson *et al.*, Phys. Rev. Lett. **97**, 31 (1983).
- [12] G. Corcella *et al.*, HERWIG 6.5 Release Note, hep-ph/0210213.
- [13] D. Amati and G. Veneziano, Phys. Lett. B **83**, 87 (1979).
- [14] D. Acosta, *et al.* (CDF Collaboration), Phys. Rev. Lett. **88**, 161802 (2002).
- [15] V.M. Abazov, *et al.* (D0 Collaboration), Phys. Rev. Lett. **101**, 182004 (2008).
- [16] P. Faccioli *et al.*, Phys. Rev. D **81**, 111502(R) (2010).
- [17] T. Aaltonen *et al.* (CDF Collaboration), Phys. Rev. Lett. **108**, 151802 (2012).
- [18] S. Chatrchyan *et al.* (CMS Collaboration), arXiv:1209.2922 [hep-ex].